Electronic Supplementary Material (ESI) for Chemical Science.
This journal is © The Royal Society of Chemistry 2022

Electronic Supplementary Information

Profiling single-molecule reaction kinetics under nanopore confinement

Wei Liu[a], Zhong-Lin Yang[a], Chao-Nan Yang[a], Yi-Lun Ying[*ab] and Yi-Tao Long[a]

Affiliations:

[a] State Key Laboratory of Analytical Chemistry for Life Science, School of Chemistry and Chemical Engineering, Nanjing University, Nanjing 210023, P. R. China.

[b] Chemistry and Biomedicine Innovation Center, Nanjing University, Nanjing 210023, P. R. China

* E-mail: yilunying@nju.edu.cn

1. Materials and Methods

1.1 Materials and Reagents

Decane (anhydrous, ⩾ 99%), KCl, ethylenediaminetetraacetic acid (EDTA), Tris(Hydroxymethyl)-aminomethane, trypsin-EDTA were purchased from Sigma-Aldrich (St. Louis, MO, USA). 1,2-Diphytanoyl-sn-glycerol-3-phosphocholine (DMPC) was obtained from Avanti Polar Lipids (Alabaster, AL, USA). Peptides $\boldsymbol{R_1}$-$\boldsymbol{R_5}$ were synthesized and purified by Sangon Biotech (Shanghai, China). K238C and wild-type (WT) pro-aerolysin were purified and activated in our laboratory. Pro-aerolysin was characterized by mass spectrum (Waters Xevo G2-QTOF, USA). K238C pro-aerolysin and Peptide $\boldsymbol{R_1}$-$\boldsymbol{R_5}$ are preserved in 50 nM dithiothreitol solution.

1.2 Nanopore Measurements

Delrin bilayer cup (Warner Instruments, Hamden, CT, USA) was used to perform the experiments. As described in our previous studies[1,2], DMPC solution was spread across a 50 μm orifice in the Delrin partition. WT or K238C aerolysin were added into the grounded *cis* chamber to form a heptameric pore. A pair of Ag/AgCl electrodes were used to apply potentials across the membrane. Peptides ($\boldsymbol{R_1}$-$\boldsymbol{R_5}$) were added into the *cis* chamber with a final concentration of 50 μM. All experiments were conducted by premixing the peptide samples with the electrolyte solution. Ionic currents were recorded using an Axopatch 200B patch-clamp amplifier (Molecular Devices, Sunnyvale, CA, USA) coupled with a Digidata 1440A A/D converter (Molecular Devices, USA). The signals were filtered at a cut-off frequency of 5 kHz at a sampling frequency of 100 kHz and acquired with Clampex 10.4 software (Molecular Devices, USA).

1.3 Data Analysis

The nanopore data was processed with home-designed PyNano[3] (www.pynanolab.com), followed by OriginLab 8.0 (OriginLab Corporation, Northampton, MA, USA). The open-pore current of K238C AeL in our experiments was 52.0 ± 0.2 pA at + 100 mV with peak-to-peak noise of 5.6 ± 0.1 pA (n = 5). Therefore, we set the current threshold of 49.0 pA in PyNano to avoid the baseline derivation.

2 Supplementary Results and Discussions

2.1 Characterization of K238C Proaerolysin

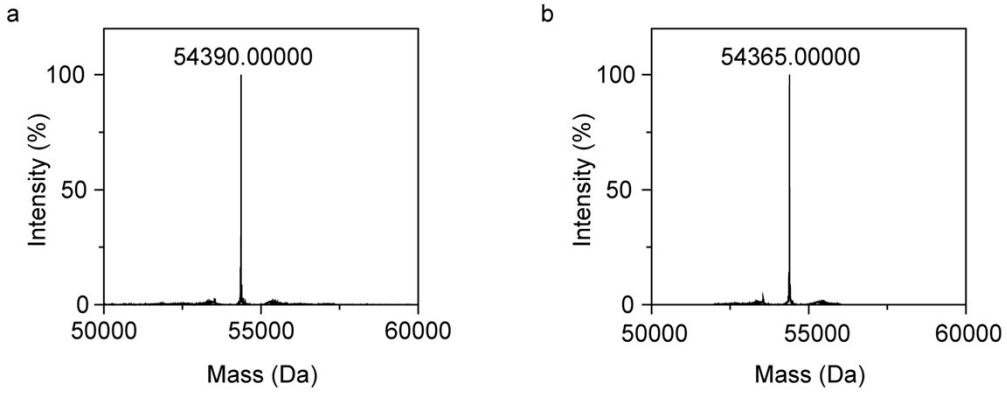

Fig. S1 Mass spectrometry of purified proaerolysin. a) WT proaerolysin; b) K238C proaerolysin. The molecular weight difference of 25.0 Da between WT and K238C proaerolysin demonstrated that the Lys (146.2 Da) was mutated into Cys (121.2 Da).

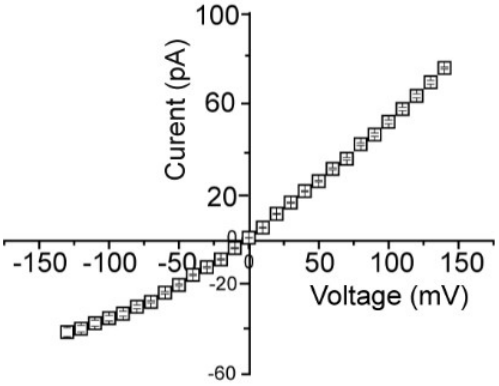

Fig. S2 I-V curves for K238C AeL. Experiments were performed in 1.0 M KCl 10.0 mM Tris, and 1.0 mM EDTA, pH 8.0. The standard deviation is based on five separate experiments.

2.2 Discrimination of Reaction Events and Non-reaction Events

When 50.0 μM $\boldsymbol{R_1}$ (EEESGSGSGSGSGSC) was introduced into the *cis* chamber, a characteristic ionic current trace occurred, indicating the chemical reaction or non-reaction occurred inside nanopore confined space (Figure S3a). According to our previous study[4], the reaction events (Type I) and non-reaction but rapid interaction with K238C site events (Type II) can be classified through the duration histograms whose logarithmic forms are fitted to Gaussian peaks (Fig. S3b). The bumping events with shorter durations are independent of the voltages (Fig. S3c) and they have been excluded in our further analysis. As $\boldsymbol{R_1}$ was driven into the WT AeL which does not contain cysteine residues, it produced only short-duration events (Fig. S4). This result further demonstrates that long-duration events (> 120 ms) should be ascribed into the forming and breaking of a single disulfide bond between $\boldsymbol{R_1}$ and K238C AeL. The exponential decreasing of duration for non-reaction events (t_{D-NR}) under increasing voltages further supports the translocation of $\boldsymbol{R_1}$ through K238C AeL (Fig. S5a).

The diameter of the K238C Aerolysin is approximately 1 nm[5]. Considering the radius of peptides[6], two peptides could not be captured at the same time. When a single peptide is captured, the probability (p) of another peptide subsequently captured could be calculated by eqn S1:

$$p = \frac{t_{D-NR}}{t_{I-NR}} \times 100\% \qquad \text{eqn S1}$$

according to Table S1, the *p-value* is smaller than 1%. Therefore, the multiple peptides to be captured simultaneously can be ignored.

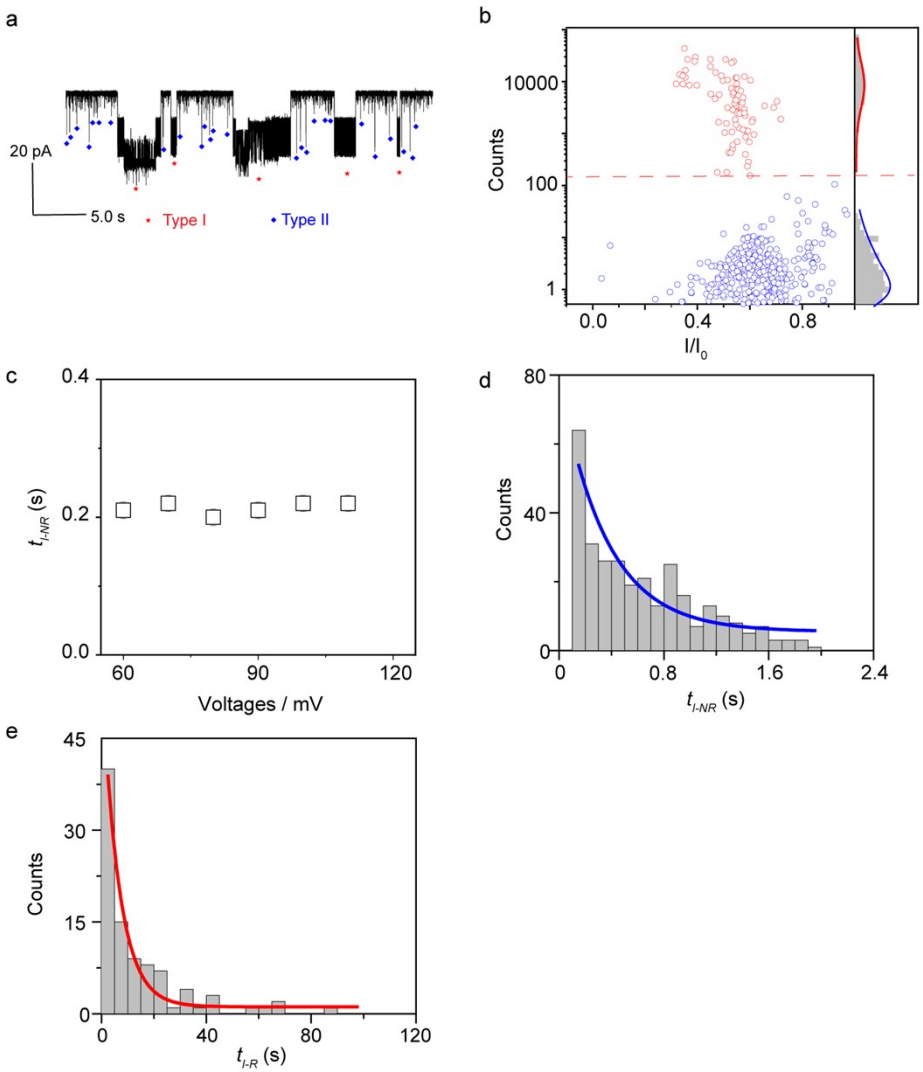

Fig. S3 Driven $\boldsymbol{R_1}$ through K238C AeL. a) The represent ionic current traces. The reaction events (Type I) are marked by red symbols, and the non-reaction events (Type II) are marked by blue symbols. The remaining events (except for Type I and Type II events) are bumping events with shorter durations. b) Scatting plots and corresponding duration histograms in logarithmic form. The red plots and blue plots represent the reaction events (Type I) and non-events (Type II), respectively. c) The voltage-independent property of durations for bumping events from + 60 mV to + 110 mV. d) Interval time histogram of non-reaction events (t_{I-NR}). e) Interval time histogram of reaction events (t_{I-R}). The duration histogram is fitted by the single exponential function. Experiments are performed under + 60 mV, in 1.0 M KCl solution, 10.0 mM Tris, and 1 mM EDTA at pH 8.0.

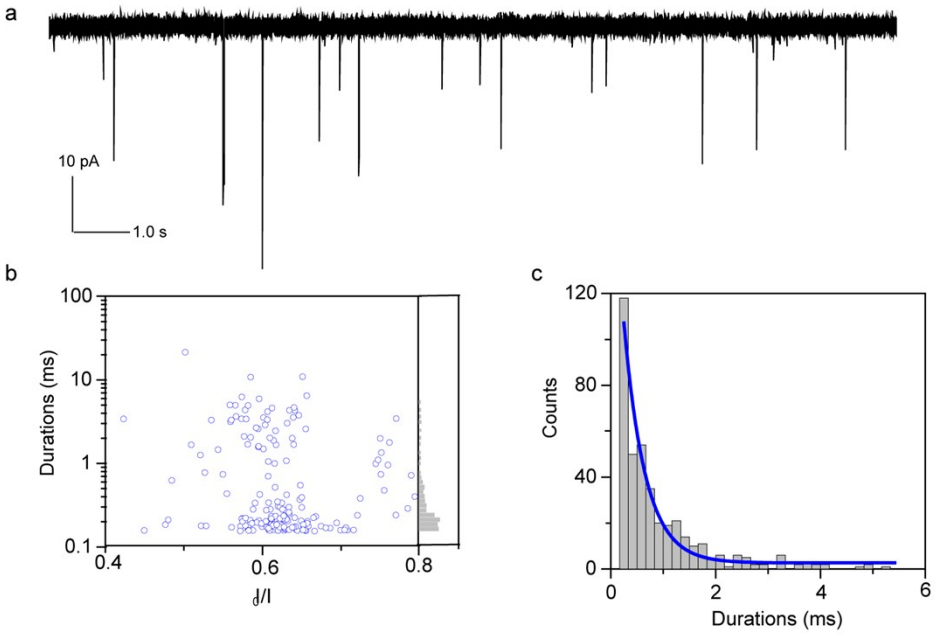

Fig. S4 The translocation of $\boldsymbol{R_1}$ through a WT AeL. a) Ionic current trace; b) Scatting plots; c) Duration histogram. The duration histogram is fitted by the single exponential function. Experiments were performed under + 60 mV in 1.0 M KCl solution, 10 mM Tris, and 1 mM EDTA (pH 8.0).

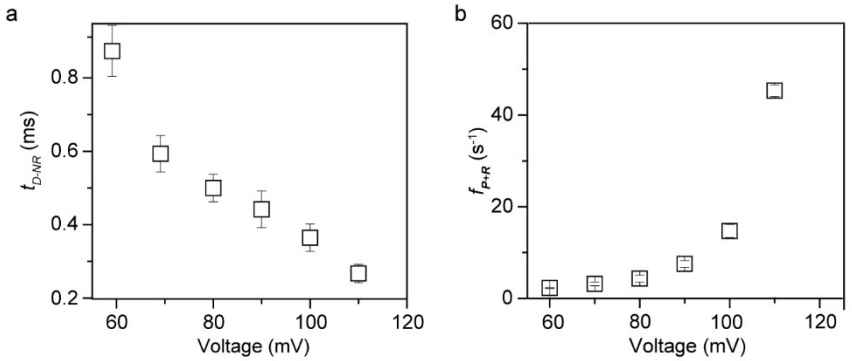

Fig. S5 The duration (t_{D-NR}) and interval time of non-reaction events of $\boldsymbol{R_1}$ in K238C AeL. a) The duration time of non-react events (t_{D-NR}) of $\boldsymbol{R_1}$ in K238C AeL under different voltages from + 60 mV to + 110 mV. b) The capture frequency of non-react events f_{P+R} of $\boldsymbol{R_1}$ in K238C AeL under different voltages from + 60 mV to + 110 mV. f_{P+R} is calculated by $f_{P+R} = \frac{1}{t_{I-NR}} = k_1[R]$. Experiments were performed in 1.0 M KCl, 10 mM Tris, and 1 mM EDTA (pH 8.0).

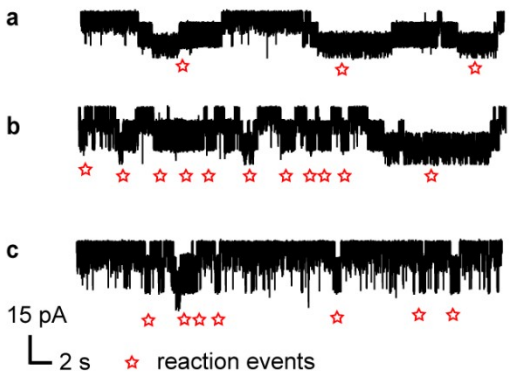

Fig. S6 The raw date of $\boldsymbol{R_1}$ react with K238C AeL nanopore under voltages of + 60 mV (a); + 80 mV (b); + 100 mV (c). The reaction events are marked by red stars.

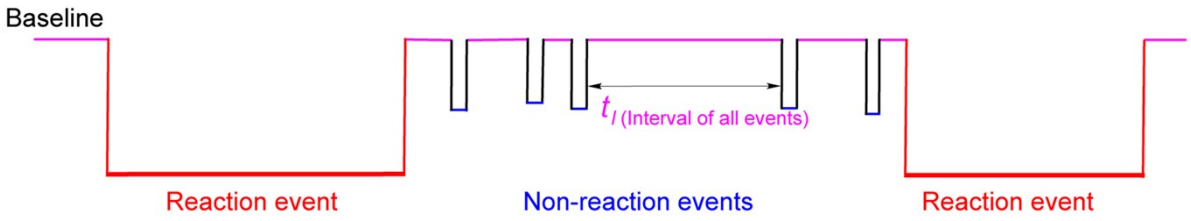

Fig. S7 Schematic illustration of t_I (Interval of both reaction or non-reaction events)

Table S1. The kinetics parameter of $\boldsymbol{R_1}$-$\boldsymbol{R_5}$ reacting with K238C AeL under different voltages

	voltage / mV	f_{PR} / s^{-1} [a]	f_{P+R} / s^{-1} [b]	ECF/% [c]	$t_{D\text{-}NR}$ / ms [d]
$\boldsymbol{R_1}$, $EEE(SG)_5SC$	+ 60	0.09 ± 0.02	0.53 ± 0.11	18.0 ± 2.0	0.86 ± 0.03
	+ 70	0.25 ± 0.07	1.45 ± 0.42	17.0 ± 3.0	0.59 ± 0.04
	+ 80	0.48 ± 0.13	2.59 ± 0.77	18.0 ± 1.0	0.50 ± 0.03
	+ 90	0.42 ± 0.05	5.81 ± 0.74	7.0 ± 0.8	0.44 ± 0.04
	+ 100	0.33 ± 0.03	12.97 ± 1.43	3.0 ± 0.6	0.35 ± 0.03
	+ 110	0.38 ± 0.02	43.56 ± 1.29	1.0 ± 0.2	0.28 ± 0.02
$\boldsymbol{R_2}$, EEESGSRSGC	+ 60	0.11 ± 0.02	1.56 ± 0.67	8.0 ± 0. 5	0.46 ± 0.02
	+ 80	0.20 ± 0.03	3.64 ± 1.22	7.0 ± 0. 7	0.22 ± 0.02
	+ 100	0.31 ± 0.04	11.23 ± 1.35	4.0 ± 0. 2	0.20 ± 0.03
	+ 120	0.12 ± 0.01	14.93 ± 1.60	1.0 ± 0.1	0.08 ± 0.01
$\boldsymbol{R_3}$, $EEG(SG)_3C$	+ 60	0.10 ± 0.01	1.01 ± 0.21	10.0 ± 0. 5	0.15 ± 0.01
	+ 80	0.14 ± 0.03	1.52 ± 0.30	8.0 ± 0.8	0.13 ± 0.01
	+ 100	0.32 ± 0.05	5.99 ± 0.67	4.0 ± 0.4	0.12 ± 0.01
	+ 120	0.27 ± 0.05	10.31 ± 1.01	2.0 ± 0.2	0.11 ± 0.01
$\boldsymbol{R_4}$, $E(SG)_4C$	+ 60	0.15 ± 0.03	1.45 ± 0.15	10.0 ± 0.5	0.18 ± 0.01
	+ 80	0.23 ± 0.06	2.73 ± 0.51	9.0 ± 0.6	0.16 ± 0.02
	+ 100	0.09 ± 0.02	3.47 ± 0.70	3.0 ± 0.3	0.15 ± 0.01
	+ 120	0.16 ± 0.04	4.88 ± 1.05	4.0 ± 0.2	0.11 ± 0.01
$\boldsymbol{R_5}$, $G(SG)_4C$	+ 60	0.24 ± 0.03	1.19 ± 0.63	23.0 ± 0.8	0.52 ± 0.03
	+ 80	0.41 ± 0.04	1.75 ± 0.88	28.0 ± 0.9	0.32 ± 0.02
	+ 100	0.16 ± 0.02	3.33 ± 0.92	5.0 ± 0.3	0.30 ± 0.03
	+ 120	0.23 ± 0.05	14.93 ± 2.03	2.0 ± 0.2	0.18 ± 0.01

[a] The reaction rate is calculated by eqn 9.

[b] $k_1[\boldsymbol{R}]$ represents the capture frequency of the reactant and is calculated by eqn 1.

[c] The ECF is calculated by eqn 2.

[d] The t_{D-NR} is analysed by ADEPT mode[7] in pynano with signal recovery.

2.3 Collision Threshold Energy of Single-Molecule Reaction

The proportion of $\boldsymbol{R_1}$ has a particular energy, at temperature T which is given by the Boltzmann's factor (assuming only translational energy along two degrees of freedom) as[8]:

$$\frac{N_E}{N} = e^{-\varepsilon_0/RT} \qquad \text{eqn S2}$$

wherein N_E of $\boldsymbol{R_1}$ has energy ≥ ε_0. The number of collisions is directly proportional to the number of molecules presenting in the solution. Moreover, the larger residence time of $\boldsymbol{R_1}$ inside a nanopore would trigger the bond-formation process at lower energy. Therefore, the ε_0 could be calculated by equation eqn S3 and S4 (for single-molecule reaction):

$$ECF = \frac{N_{PR}}{N} = \frac{N_E}{N} = e^{-\varepsilon_0/RT} \qquad \text{eqn S3}$$

$$\varepsilon_0 = -k_B T ln(ECF) \qquad \text{eqn S4}$$

2.4 Driven R_2, R_3 R_4, and R_5 through K238C AeL

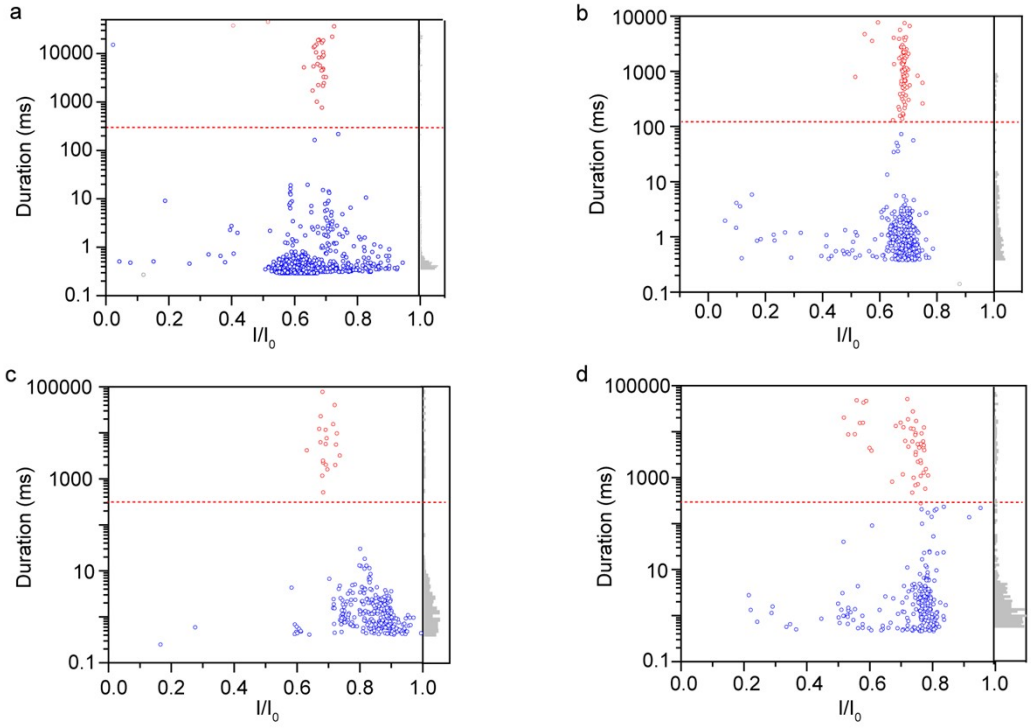

Fig. S8 Scatting plots of R_2 (a), R_3 (b), R_4 (c), and R_5 (d) with K238C AeL at + 60 mV. Experiments were performed in 1.0 M KCl solution, 10.0 mM Tris, and 1.0 mM EDTA at pH 8.0. The red plots and blue plots represent the reaction events and non-reaction events, respectively. The duration threshold sets at 300 ms for R_2 (a), 120 ms for R_3 (b), 300 ms for R_4 (c), and 300 ms for R_5 (d), respectively. The short bumping events have been excluded.

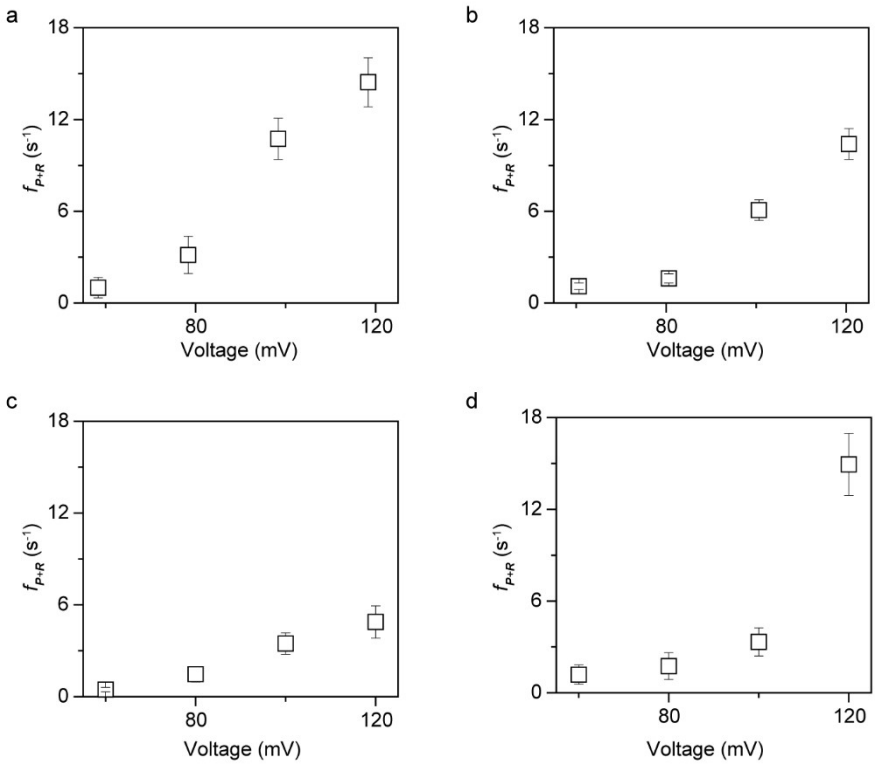

Fig. S9 The capture frequency of non-react events (f_{P+R}) of $\boldsymbol{R_2}$ (a) $\boldsymbol{R_3}$ (b) $\boldsymbol{R_4}$ (c) and $\boldsymbol{R_5}$ (d) in K238C AeL under different voltages from + 60 mV to + 120 mV. f_{P+R} is calculated by $f_{P+R} = 1/t_{I-NR}$. Experiments were performed in 1.0 M KCl solution, 10.0 mM Tris, and 1.0 mM EDTA at pH 8.0.

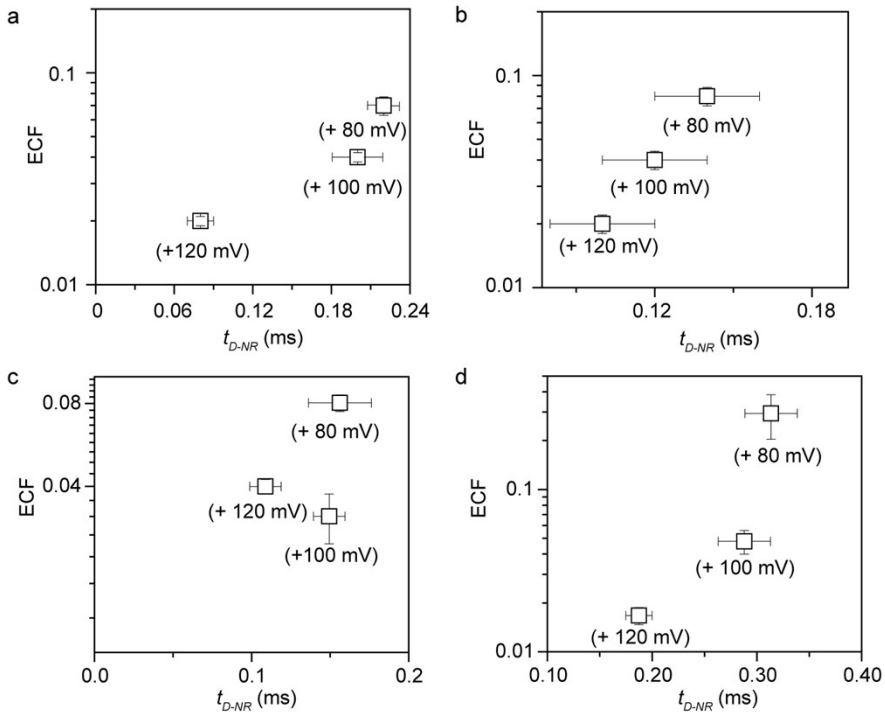

Fig. S10 The relationship between the duration time of non-reaction events (t_{D-NR}) of $\boldsymbol{R_2}$ (a), $\boldsymbol{R_3}$ (b), $\boldsymbol{R_4}$ (c), $\boldsymbol{R_5}$ (d) and ECF under voltages from + 80 mV, + 100 mV and + 120 mV.

2.5 Single Bond Breaking Process under Nanopore Confinement

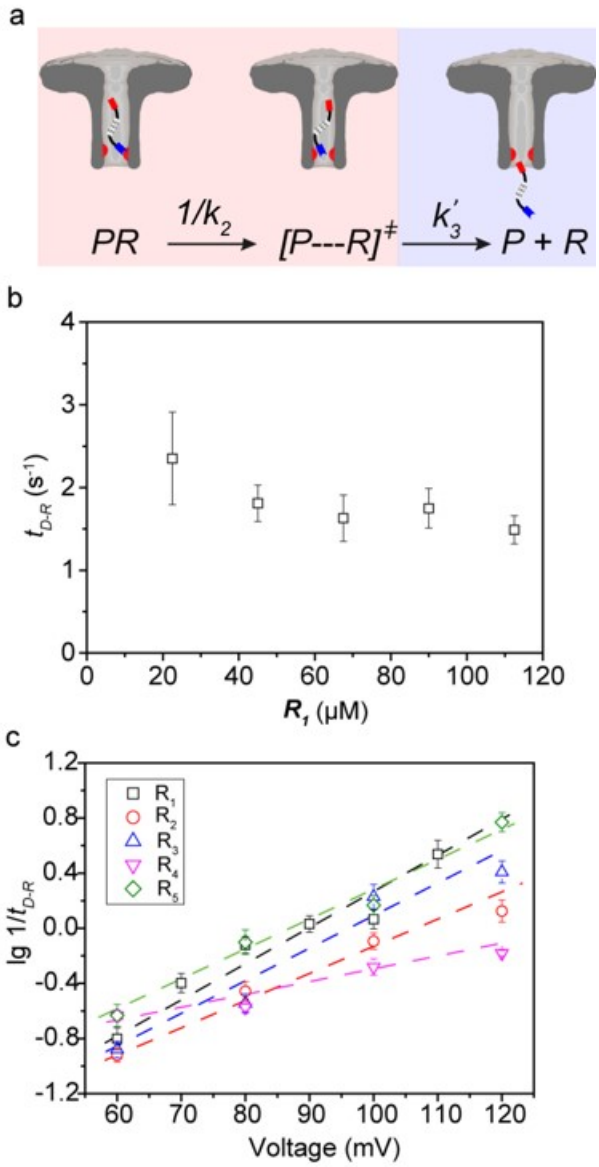

Fig. S11 Kinetics insight of the bond breaking process. a) The proposed three-state model to describe the bond-breaking process. $1/k_2$ represents the bond-breaking constant and k_3' represents the escape rate of ***R*** from a reaction site to the *trans* side. b) The duration time of reaction events (t_{D-R}) of $\boldsymbol{R_1}$ under different concentrations. c) The logarithm of bond breaking constant ($\lg(1/t_{D-NR})$) of $\boldsymbol{R_1}$-$\boldsymbol{R_5}$ under different voltages.

References

1 C. Cao, D. -F. Liao, J. Yu, H. Tian and Y. -T. Long, *Nat. Protocols*., 2017, **12**, 1901-1911.

2 B. Zhou, Y. Wang, C. Cao, D. Li and Y. -T. Long, *Sci. China Chem.*, 2018, **61**, 1385-1388.

3 S. -C. Liu, B. -K. Xie, C. -B. Zhong, J Wang, Y.-L. Ying, and Y. -T Long, *AIP Rev. Sci. Instrum.*, 2021, **92**, 121301.

4 C. Cao, Y. -L. Ying, Z. -L. Hu, D. -F. Liao, H. Tian and Y. -T. Long, *Nat. Nanotech*, 2016, **11**, 713-718.

5 C. Cao and Y. -T. Long, *Acc. Chem. Res.*, 2018, **51**, 331-341.

6 J. L. Finney and A. K. Soper, *Chem. Soc. Rev.*, 1994, **23**, 1-10.

7 J. H. Forstater, K. Briggs, J. W. Robertson *et al*, *Anal. Chem.*, 2016, **88**, 11900–11907.

8 S. K. Upadhyay, Chemical Kinetics and Reaction Dynamics, Theories of Reaction Rate, Chapter 4, 2007, pp. 83-89.